Behavior of noncircular tunnels excavated in stratified rock masses – Case of underground coal mines

Ngoc Anh Do, Daniel Dias, van Diep Dinh, Tien Tung Tran, van Canh Dao, Viet Doan Do, Phuc Nhan Nguyen

▶ **To cite this version:**

Ngoc Anh Do, Daniel Dias, van Diep Dinh, Tien Tung Tran, van Canh Dao, et al.. Behavior of noncircular tunnels excavated in stratified rock masses – Case of underground coal mines. Journal of Rock Mechanics and Geotechnical Engineering, 2019, 11 (1), pp.99-110. 10.1016/j.jrmge.2018.05.005 . hal-02019384

HAL Id: hal-02019384
https://hal.science/hal-02019384

Submitted on 21 Oct 2021

HAL is a multi-disciplinary open access archive for the deposit and dissemination of scientific research documents, whether they are published or not. The documents may come from teaching and research institutions in France or abroad, or from public or private research centers.

L'archive ouverte pluridisciplinaire **HAL**, est destinée au dépôt et à la diffusion de documents scientifiques de niveau recherche, publiés ou non, émanant des établissements d'enseignement et de recherche français ou étrangers, des laboratoires publics ou privés.

Distributed under a Creative Commons Attribution - NonCommercial 4.0 International License

Version of Record: https://www.sciencedirect.com/science/article/pii/S167477551830009X
Manuscript_217aba7f04a02f3a3c394e6c0d1fb9c7

Behavior of Noncircular Tunnels Excavated in Stratified Rock Masses – Case of Underground Coal Mines

Ngoc Anh Do[1], Daniel Dias[2,3], Van Diep Dinh[1], Tien Tung Tran[1], Van Canh Dao[1], Viet Doan Dao[1], Phuc Nhan Nguyen[1]

[1]*Hanoi University of Mining and Geology, Faculty of Civil Engineering, Department of Underground and Mining Construction, Hanoi, Vietnam*
[2] *School of Automotive and Transportation Engineering, Hefei University of Technology, Hefei, 230009, China*
[3]*Laboratory 3SR, Grenoble Alpes University, Grenoble, France*

ABSTRACT. The amount of tunnels excavated along stratified/sedimentary rock masses in the Quangninh coal area is gradually increasing. Rock mass in Quangninh is characterized by beddings between rock layers. The behavior of stratified rock masses surrounding tunnels depends on both the intact rock and the bedding between rock layers. The main characteristics of stratified rock masses which need to be considered are therefore their heterogeneity and their anisotropy. Depending on the dip angle of rock layers, movements and failure zones developed surrounding tunnels can be asymmetrical over the vertical axis of tunnel. This asymmetry causes adverse behaviors of the tunnel structures.
The objective of this study is to highlight convergence displacements and yielded zones developed in rock masses surrounding noncircular tunnels in Quangninh coal mine area using a finite element method. The presence of bedding joints is explicitly simulated. The numerical results indicated that with the bedding joints dip angle increase, the stress asymmetry over the tunnel vertical axis increases. It gradually leads to an asymmetry of the failure zone surrounding the tunnel. An increase of rock mass quality means a decrease of the rock mass sensitivity to the discontinuities. In addition, a dip angle of the bedding joints of approximately 45 degrees could be considered as the critical angle for which the rock mass mechanism changes between sliding and bending.

Keywords: Tunnel; Bedding; Stratification; Anisotropic; Heterogeneity.

1. Introduction

In the Quangninh province (Vietnam), the number of open pit mines is decreasing and are gradually replaced by underground mines. The amount of tunnels in coal mines is therefore constantly increasing. Generally, rock masses in Quangninh are characterized by joints/beddings between rock layers. Unlike for intact rock, the behavior of stratified rock masses surrounding tunnels depends on both the intact rock and on the joints/beddings between rock layers behaviors. Generally, dip angle of bedding varied from 0^0 to 90^0 corresponding to respectively a horizontal and a vertical stratification. The main characteristics of the stratified rock masses in Quangninh coal mines are therefore their heterogeneity and their anisotropy.

In the literature, the effect of beddings on the behavior of rock mass is usually considered using explicit or implicit methods. With explicit methods, bedding joints are explicitly simulated using joint elements (Jia and Tang 2008; Fortsakis et al. 2012; He at al. 2012; Małkowski 2015; Yang et al. 2013; Panthee et al. 2016). In Jia and Tang (2008), a finite element code was used to numerically investigate the influence of the joints dip angles and of the lateral earth pressures factor on the stability of tunnels. The results indicated that both the

© 2018 published by Elsevier. This manuscript is made available under the CC BY NC user license
https://creativecommons.org/licenses/by-nc/4.0/

dip angle and the lateral earth pressure coefficient have a considerable impact on the tunnel behavior. They concluded that in the case of horizontal layered joints, the failure mode is of ‘‘rock beam’’ type; for joints with dip angle between 30 degrees and 45 degrees, the failure mode is sliding of sidewall and detaching, flexing and breaking of the layered rock mass near the tunnel shoulder; for joints with a larger dip angle, the failure mode is sliding of the rock mass along the joints interface. In their study, the gravity of rock mass was however not considered. In addition, it is impossible to make a general recommendation of the effect of joints on the tunnel behavior due to the limited number of performed calculations. He et al. (2012) adopted the distinct element method (UDEC software) to highlight the behavior of a tunnel under the effect of bedding planes. The authors recommended that an asymmetric support structure should be used to reinforce the geologically inclined bedding asymmetric load. Recently, relatively comprehensive studies of the anisotropic behavior of stratified rock mass in tunnelling conducted by Fortsakis et al. (2012) and Wang et al. (2012) pointed out the importance of the stratification planes and of the rock mass quality affecting the radial displacements around the tunnel. Only circular tunnels were considered in these studies. Małkowski (2015) numerically investigated the effect of the constitutive model and of the rock mass stratification on the rock mass deformation around the tunnels. They demonstrated the inaccuracies of modeling the rock mass by using an elastic constitutive model. In other words, it is necessary to use elasto-plastic models to accurately simulate the rock mass behavior. In this study, a horizontal stratification was only considered.

With implicit methods, bedding joints are implicitly considered as transversely isotropic material (Fortsakis et al. 2012; Tran et al. 2015; Rafeh et al., 2015; Wang et al., 2015; Bobet, 2016). By comparing the displacement developed in a transversely isotropic rock mass with the one obtained in the corresponding anisotropic rock mass, Fortsakis et al. (2012) emphasized that simulating a rock mass as a transversely isotropic material does not lead to the same displacement field as in anisotropic rock mass. This difference is due to the sliding effect along the bedding joints. It is therefore evident that an explicit simulation of the joints is necessary to introduce for stratified rock masses.

Obviously, most of previous researches focused on investigating the behaviour of circular tunnels considering the influence of inclined stratification (Jia and Tang, 2008; Fortsakis et al, 2012; He et al., 2012; Wang et al., 2012, etc.) or the behaviour of noncircular tunnels excavated in horizontal stratification (Małkowski, 2015). So far, the effect of inclined beddings in rock mass has not been often mentioned and has not been clarified in the literature.

This paper aims, therefore, to highlight the effect of inclined beddings in rock masses and support structures on the displacement field developed around noncircular tunnels using a finite element method (FEM). The presence of bedding joints is explicitly simulated. The numerical results indicated that with the bedding joints dip angle increase, the stress asymmetry over the tunnel vertical axis increases. It gradually leads to an asymmetry of the failure zone surrounding the tunnel. An increase of rock mass quality means a decrease of the rock mass sensitivity to the discontinuities. In addition, a dip angle of the bedding joints of approximately 45 degrees could be considered as the critical angle for which the rock mass mechanism changes between sliding and bending.

2. Evaluation of rock mass properties

In the numerical calculations, a constitutive model using the Hoek-Brown failure criterion (Hoek et al. 2002) was adopted for the rock mass surrounding tunnels (Marinos 2014; Małkowski 2015). The joints strength was evaluated through the Barton and Bandis failure criterion (Barton and Bandis 1990). Both above constitutive models are widely applied when tunnels are excavated in rock mass (Fortsakis et al 2012; Małkowski 2015). Typical parameters of the Quangninh coal area (IMSAT 2012) were considered in this study.

A range of Geological Strength Index (GSI) values changing from 10 to 80 has been adopted which covers rock mass conditions varying from very poor to very good. The uniaxial compressive strength of intact rock (σ_{ci}) was chosen in a range from 10 MPa to 100 MPa, the modulus ratio MR = 500 and the geomaterial constant m_i = 7. The deformation modulus of intact rock E_i is determined as follows (Hoek et al. 2002):

$$E_i = MR\ \sigma_{ci} \tag{1}$$

Where σ_{ci} is the uniaxial compressive strength of intact rock.

The deformation modulus of rock mass ($E_{m,ref}$) (Hoek et al. 2002) was calculated on the basis of the following relationship:

$$E_{m,ref} = E_i\left(0.02 + \frac{1 - D/2}{1 + e^{((60+15D-GSI)/11)}}\right) \tag{2}$$

Where E_i is the deformation modulus of intact rock, D is disturbance factor.

The shear modulus of intact rock (G_i) and rock mass ($G_{m,ref}$) are estimated as follows:

$$G_i = \frac{E_i}{2(1+\mu)}$$
$$G_{m,ref} = \frac{E_{m,ref}}{2(1+\mu)} \tag{3}$$

Where μ is the Poisson's ratio of rock.

Assuming that the rock mass is a combination of intact rock and discontinuities, the deformability properties of these elements are calculated through the following equations (Barton 1972; Goodman 1989; Fortsakis et al. 2012):

$$\frac{1}{E_{m,ref}} = \frac{1}{E_{m,\text{int}}} + \frac{1}{s_p k_n}$$
$$\frac{1}{G_{m,ref}} = \frac{1}{G_{m,\text{int}}} + \frac{1}{s_p k_s} \tag{4}$$

where $E_{m,ref}$ and $G_{m,ref}$ are respectively the reference rock mass deformation and the shear modulus, $E_{m,int}$ and $G_{m,int}$ are the deformation and the shear modulus of the internal rock mass, s_p is the bedding width and k_n and k_s are the normal and the shear stiffness of the discontinuities.

The values of k_n and k_s can be calculated based on results of laboratory tests. In this study, because such data are not available, these values were calculated based on Equation (4) as follows (Fortsakis et al. 2012):

$$k_n = \frac{E_{m,L}E_i}{(E_i - E_{m,L})s_p}$$
$$k_s = \frac{G_{m,L}G_i}{(G_i - G_{m,L})s_p} \tag{5}$$

where E_i, G_i are the Young's modulus and the shear modulus of the intact rock and $E_{m,L}$, $G_{m,L}$ are the Young's modulus and the shear modulus of the rock mass determined with the GSI_{tab}. GSI_{tab} is the GSI value of the first row of the joint surface conditions illustrated in the

GSI chart (Hoek et al. 2002). This case corresponds to intact or massive rock with few widely spaced discontinuities.

The joint wall compressive strength (JCS) and joint roughness strength (JRC) were determined using the rock joint classification condition suggested by Fortsakis et al. (2012) (see **Table 1**).

Table 1. Parameters of rock discontinuity

No	Discontinuity surface quality	JRC	JCS
1	Very poor	2	$0,1\sigma_{ci}$
2	Poor	6	$0,3\sigma_{ci}$
3	Fair	10	$0,5\sigma_{ci}$
4	Good	18	$0,6\sigma_{ci}$

Because the support structure has a great impact on the behavior of the tunnel excavated in stratified rock mass, two cases of tunnels with and without support structure have been investigated in this study.

3. Numerical model

FEM was used in this study to model the influence of rock joint on the stability of tunnel and subsequent estimation of parameters which influence on the deformation and development of yielded zone induced in rock mass. FEM has been used previously by many researchers (Fortsakis 2012; Małkowski 2015; Panthee et al. 2016). Firstly, monitoring data (displacements) induced in the surrounding rock mass due to the Tunnel N-6-8 excavation in the Duonghuy coal mine (Quangninh, Vietnam) was used to validate the numerical model. The tunnel shape is presented in **Fig. 1**. The tunnel dimensions are 4.03 m in width and 3.24 m in height. This tunnel was excavated along a coal seam (**Fig. 2**). This tunnel was used to exploit the coal and transport it to outside. The tunnel is located at the depth of 150 meters from the ground surface. Properties of the rock mass and of the discontinues surrounding the Tunnel N-6-8 are described in **Table 2 and Table 3**. It should be mentioned that parameters JCS and JRC of joint are determined on the basis of properties of the weaker rock contact. They were determined through both in-site and laboratory tests. This tunnel was supported by steel ribs, their properties are given in **Table 4**. The steel ribs are installed right after each excavation cycle and at the maximum distance of 0.7m from the tunnel face.

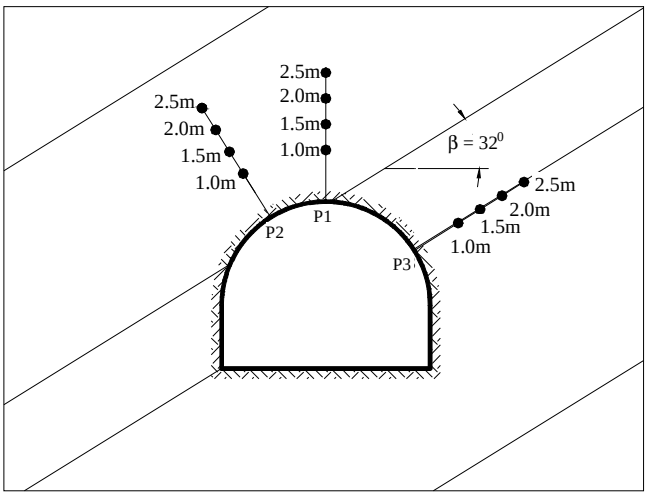

Fig. 1. Location of monitoring extensometers installed in Tunnel N6-8

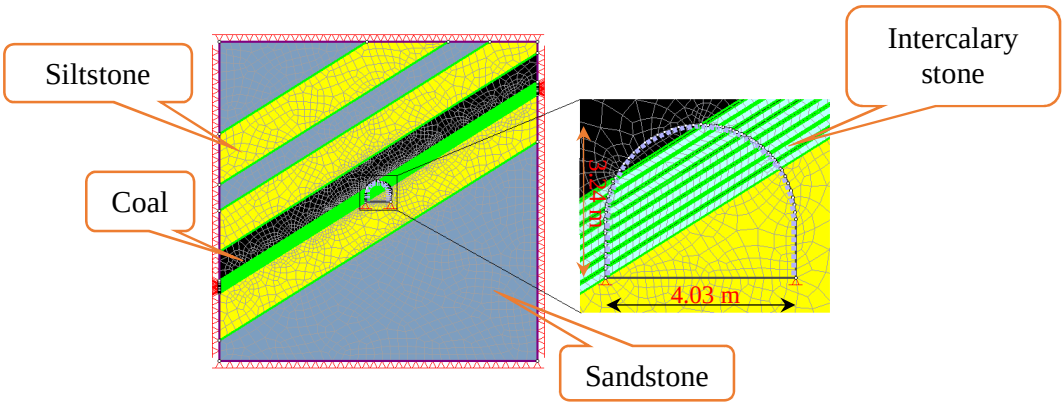

a) 2D numerical model using the RS2 software

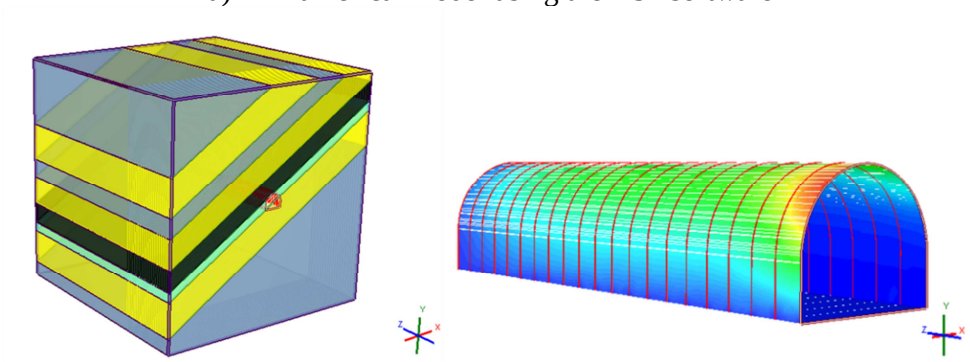

b) 3D numerical model using the RS3 software

Fig. 2. Adopted numerical models for the N6-8 Tunnel (Rocscience)

Three extensometers have been installed in rock mass from the tunnel wall to monitor the displacements induced in rock mass after the excavation (see **Fig. 1**). Each extensometer has 4 rods which have different lengths of 1m, 1.5m, 2m, 2.5m measured from the tunnel wall. The displacements induced in rock mass were frequently monitored during six months until the tunnel boundary reached a stable state.

Both 2D and 3D numerical models built using the RS2 and the RS3 softwares (Rocscience 2016), respectively, were used to make a comparison with monitored data obtained from the tunnel site (**Fig. 2**). In the 2D model, a relaxation process using the softening method was applied to take into account of the pre-displacements in rock mass surrounding the tunnel after excavation and before the steel rib installation (Do et al. 2014). A reduced deformation modulus (E_{red}) of 70% of the initial value (E) was adopted on the basis of a back analysis done on the pre-displacement value monitored at the top of the tunnel before the installation of the tunnel support structure.

Table 2. Parameters of rock layers in Tunnel N6-8

Layers	Density	Uniaxial compressive strength σ_{ci} (MPa)	GSI	Cohesion C (MPa)	Internal friction angle φ (degrees)	Young modulus E (MPa)
Sandstone	2.65	86.62	60	1.33	40.59	11,585
Siltstone	2.65	46.48	50	0.69	31.95	4,772
Coal	1.4	20	20	0.19	14.23	556
Intercalary stone	2	25	45	0.392	27.34	2,624

Measured displacements along three extensometers installed at tunnel site are presented in **Table 5**. **Fig. 3** shows the yielded zone developed surrounding the tunnel obtained from 2D numerical model. It can be seen that the ends of extensometers are outside the yielded zone of the rock mass. The comparison between the numerical and experimental results is presented in **Table 5**.

Table 3. Stiffness of joints in numerical model for the case of Tunnel N6-8

Rocks in contact	JCS (MPa)	JRC
Sandstone - Siltstone	23.24	10
Siltstone - Intercalary stone	7,5	6
Intercalary stone - Coal	2.0	2
Coal - Siltstone	2.0	2

Table 4. Properties of the steel ribs

Properties	Values
Height of section (m)	0.171
Cross section area (m^2)	0.002173
Inertia moment (m^4)	$2.43\ 10^{-6}$
Young's modulus (MPa)	210,000
Poisson ratio (υ)	0.25

Table 5. Comparison between monitoring data and numerical models (2D and 3D)

Distance from the tunnel wall (m)	Displacement in rock mass (m)								
	Measured data			2D model			3D model		
	P1	P2	P3	P1	P2	P3	P1	P2	P3
1	0.080	0.095	0.015	0.060	0.088	0.012	0.048	0.094	0.018
1.5	0.045	0.090	0.015	0.047	0.066	0.008	0.038	0.069	0.011
2	-	0.040	0.015	0.033	0.045	0.008	0.030	0.050	0.008
2.5	0.02	0.040	0.015	0.027	0.028	0.008	0.025	0.039	0.004
Maximum displacement (D_{max}) (m)	0.080	0.095	0.015	0.060	0.088	0.012	0.048	0.094	0.018
D_{ratio}	-	-	-	0.75	0.93	0.80	0.60	0.99	1.20

Note: $D_{ratio} = D_{max\text{-}model}/D_{max\text{-}measured}$ (where: $D_{max\text{-}model}$ is the maximum displacement obtained in numerical models at each location (P1, P2 or P3); $D_{max\text{-}measured}$ is the maximum displacement observed in tunnel site at each location (P1, P2 or P3)).

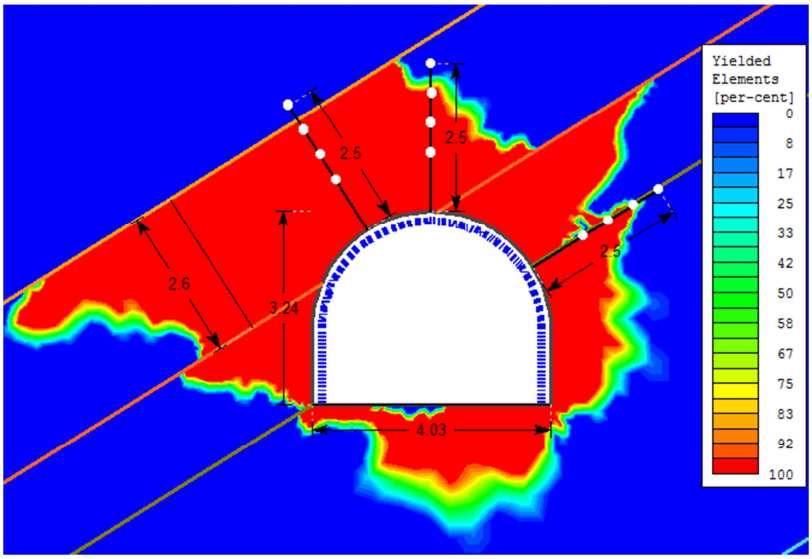

Fig. 3. Distribution of yielded zone surrounding the tunnel (2D model)

It can be seen that the 2D numerical model gives displacements which are more or less similar to those obtained in the 3D numerical model and both numerical models are relatively consistent with the monitored data. D_{ratio} values for both numerical models (2D and 3D) are close to unity, especially at point P2. The higher difference between the results of numerical models and monitored data is seen at point 3. This can be related to the fact that this borehole is parallel to the rock mass joint direction (see Figs 1 and 3). The measurements of the extensometer can therefore be disturbed by the joint at this point. Without considering the result at point 3, it is reasonable to conclude that the 2D numerical model using the relaxation process with joint elements between rock layers can be efficiently used. 2D numerical models will be therefore used in the following sections for the parametric analysis.

4. Tunnels without support

In this section, numerical analyses of tunnels without support structure in plane strain conditions have been conducted using the RS2 software (Rocscience). The aim is to highlight the effect of joints parameters on the rock mass behavior surrounding the tunnel in terms of induced displacements and stresses.

The section used is not the same as in the first part of the work. A typical section which is usually used in the Quangninh coal mines was adopted here. The tunnel cross section was assumed as an arch-profile crown and vertical sidewalls with dimension of 4.5m wide and 3.5 m high. A depth of 300 meters from the ground surface has been chosen because this depth is now widely observed in the Quangninh coal mine area. Typical rock mass parameters including the intact rock and the discontinuities in the Quangninh coal mine area were adopted in this study (see **Table 6**) (IMSAT 2012).

Table 6. Rock mass and joint parameters

Descriptions	Values
Rock mass material	
Modulus ratio MR	500
Unit weight γ(kN/m^3)	24
Poisson's ratio of rock, μ	0.25
Uniaxial compressive strength of intact rock σ_{ci} (MPa)	10; 30; 50; 70; 100

GSI_{tab}	35; 50; 75; 85
GSI (GSI_{tab})	20 (35,50); 40 (50,75); 60 (75,85); 80 (85)
Discontinuities/Joints	
Dip angle of rock layers β (degrees)	0^0; 30^0; 45^0; 60^0; 90^0
JCS (GSI_{tab})	$0.1\sigma_{ci}$ (35); $0.3\sigma_{ci}$ (50); $0.5\sigma_{ci}$ (75); $0.6\sigma_{ci}$ (85)
JRC (GSI_{tab})	2 (35); 6 (50); 10 (75); 18 (85)
Other parameters	
Lateral earth pressure coefficient K_0	0.25; 0.5; 1; 1.5; 2
Tunnel depth H (m)	100, 300

The first calculation step of the numerical excavation process consists in setting up the initial stress state taking into consideration the vertical stress under the effect of the gravity field. The ratio between lateral and vertical stresses is assumed to be K_0=0.5 for the reference case. For comparison, there are no joints in the first model. In the other models, there are bedding joints at a dip angle of β=0^0, 30^0, 45^0, 60^0, 90^0 with 0^0 and 90^0 indicating the horizontal and vertical layers, respectively. The joints were modelled as parallel surfaces in the internal rock mass. The distance between joints is equal to 1.0 meter. On the basis of a parametric analysis, numerical models with dimensions of 32m x 32m were adopted to avoid the effect of boundary condition (**Fig. 4**).

The other discontinuities strength parameters were chosen depending on the rock surface condition. The values of the joint roughness coefficient (JRC) changed from 2 (very poor) to 18 (very good). The joint compressive strength (JCS) varied from $0.1\sigma_{ci}$ (very poor) to $0.6\sigma_{ci}$ (very good) (Fortsakis et al. 2012). The GSI value is assumed to change from 10 (very poor) to 80 (very good). All rock masses and discontinuities parameters are presented in **Table 6**. In total, 800 calculations were done, thus covering most of the possible situation that could be encountered in practice of tunnel excavated in stratified rock mass in Quangninh coal mine area.

This section deals with the variations of the convergence displacements of the tunnel wall after excavation considering the influence of the bedding angle, of the joint parameters and of the rock mass quality. These variations were determined at the final state when the unsupported tunnels have reached a steady state. To investigate the effect of joints/beddings on the displacement of the tunnel boundary, 5 observation points were chosen as seen in **Fig. 5**.

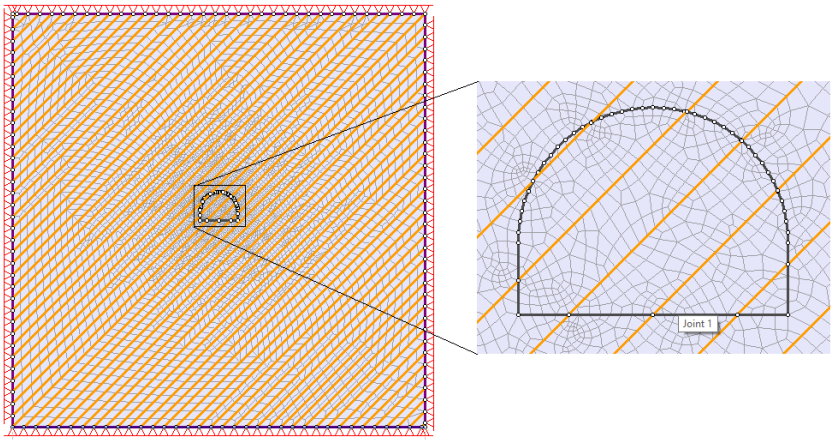

Fig. 4. Layout of numerical model

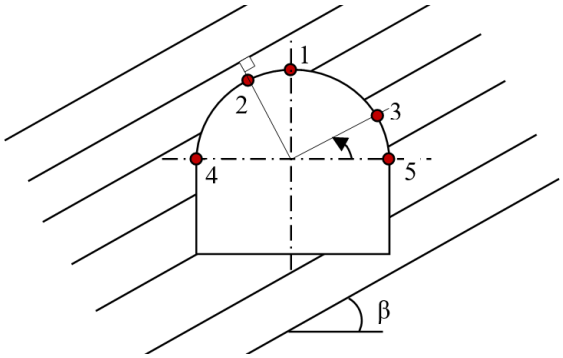

Fig. 5. Location of observation points on the tunnel boundary

Fig. 6 presents the yielded zones distribution after excavation in the case of GSI = 40, GSI_{tab} = 50, σ_{ci} = 30 MPa, K_0 = 0.5. These parameters are the ones of the reference case in this study. For intact rock masses without joints, the yielded zone is smaller than the one observed in the case of stratified rock masses. In addition, the stress distribution around the tunnel excavated in an isotropic rock mass and the case of horizontal and vertical stratification is symmetric. However, for the case of inclined stratified rock mass, with the increase of the dip angle, the asymmetry of the yielded zone developed increases gradually. It is reasonable to conclude that the influence of the stratification on the rock mass behavior surrounding the tunnel after excavation is significant and must be taken into consideration.

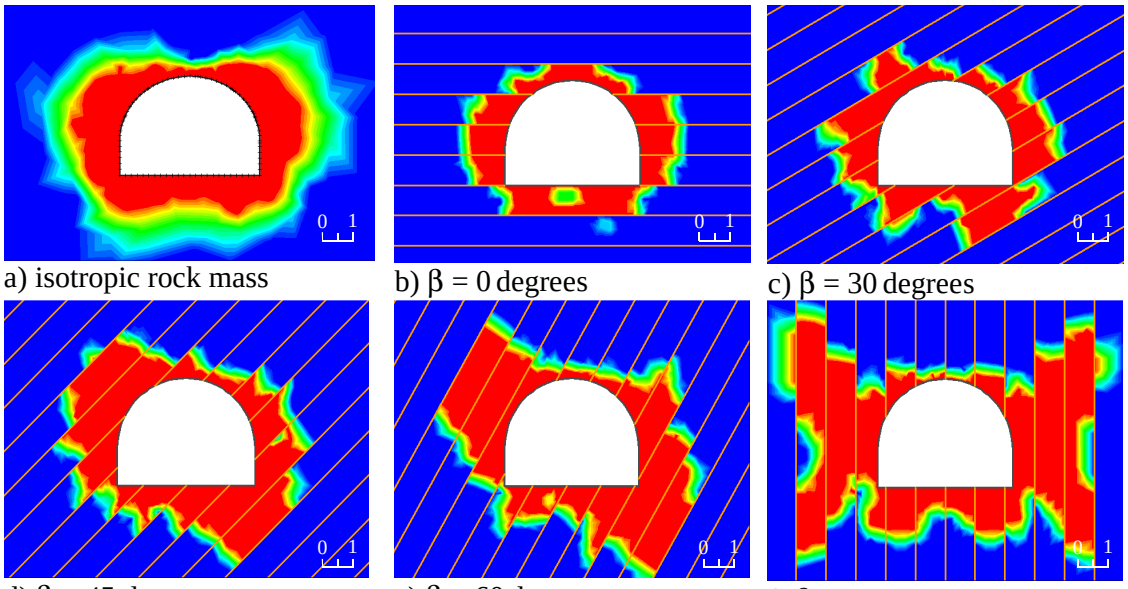

Fig. 6. Yielded zones around tunnels (*GSI* = 40, GSI_{tab} = 50 and σ_{ci} = 30 MPa) for the case of unsupported tunnel

In order to investigate the effect of the dip angle on rock mass behavior, the ratio u_β/u_0 has been adopted. The values of u_β and u_0 are the convergence displacements determined at points 1, 4 and 5 when the dip angles are larger than zero and equal to zero, respectively. The distribution of the ratio u_β/u_0 as a function of the dip angle β for points 1, 4 and 5 is illustrated in **Fig. 7**. It should be noted that the results presented in **Fig. 7** includes all considered GSI values. Generally, the higher the dip angle, the larger the scatter of the ratio u_β/u_0. In other words, the convergence displacements developed at two sides of tunnel (points 4 and 5) are highly affected by the dip angle of rock layers. It is also interesting to note that the ratio u_β/u_0 is usually larger than the unity which means that the convergence displacements induced in

the inclined layered rock masses are usually larger than the ones obtained for horizontally layered rock masses.

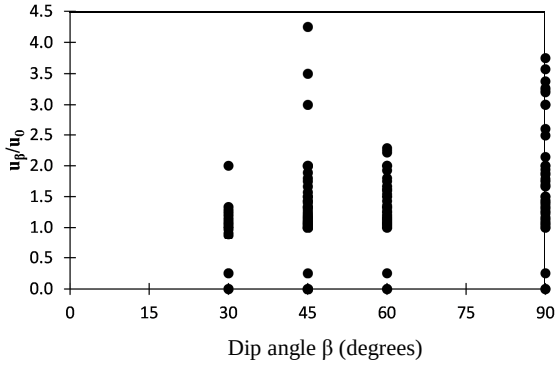

Fig. 7. Distribution of the ratio u_β/u_0 as a function of dip angle (β) for the case of an unsupported tunnel without differentiation of GSI values

Using the same data from **Fig. 7**, **Fig. 8** presents the differentiation of the GSI cases influencing on the u_β/u_0 ratio at points 1, 4 and 5. It can be seen that the smaller the GSI value, the more dependence of u_β/u_0 ratio on the dip angle of rock layers. With GSI values of 60 and 80, the scatter of u_β/u_0 ratio depending on the dip angle of rock layer is more or less similar.

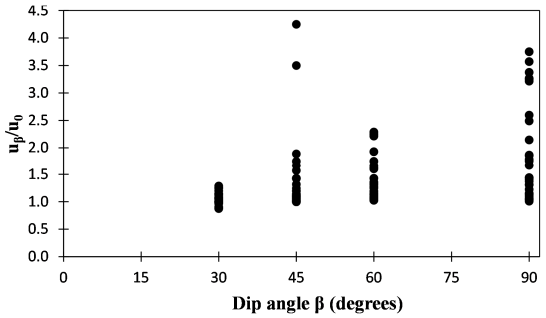

a) GSI = 20

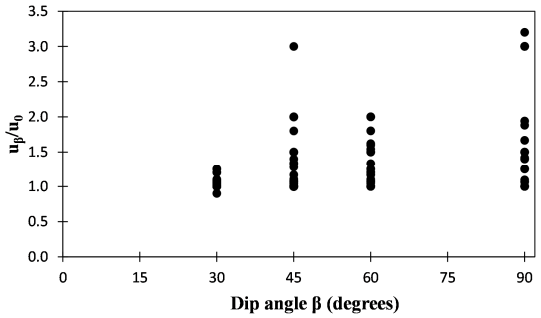

b) GSI = 40

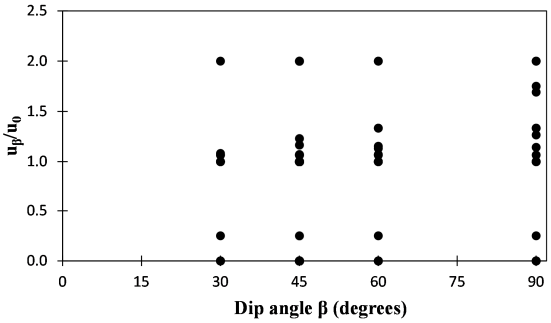

c) GSI = 60

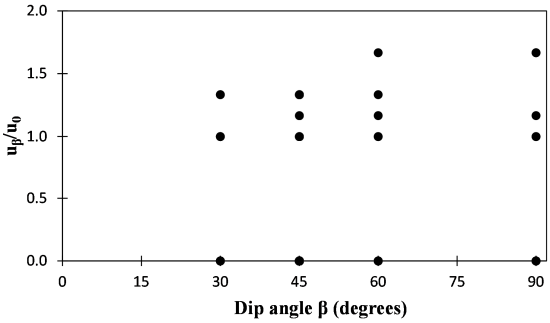

d) GSI = 80

Fig. 8. Distribution of the ratio u_β/u_0 as a function of dip angle (β) for the case of an unsupported tunnel with differentiation of GSI values

The values of u_β/u_0 significantly depend also on the rock mass quality as presented in **Fig. 9**. At tunnel crown (point 1), it can be seen that the scatter of the ratio u_β/u_0 tends to decrease as the GSI values increases. Indeed, an increase of the GSI value also means an improvement

of the rock mass quality and a decrease of the rock mass sensitivity to the discontinuities. The same results are also observed for points 4 and 5.

As for points 2 and 3, the dependence of the ratio u_β/u_0 on GSI value is not the same as at point 1. The ratio u_β/u_0 reaches the maximum value and its maximum scatter for a *GSI* value of 40 corresponding to a medium rock mass quality. In other cases, for a *GSI* value of 20 (poor rock mass), or *GSI* values higher than 60 (good rock masses), a decrease of the scatter of the ratio u_β/u_0 is observed. It is therefore reasonable to state that the ratio u_β/u_0 strongly depends of the discontinuity in the case of medium rock masses. This dependency decreases in the case of (1) highly jointed rock masses and/or poor joints condition; (2) rarely jointed rock mass and/or good joints condition.

In order to highlight the asymmetry of convergences, the deviation δ defined as the difference between the convergences at points 2 and 3 is presented in **Fig. 9d**. A significant dependency of the δ value on the *GSI* can be seen. The higher the *GSI* value, the smaller the deviation δ. The deviation of convergences at two sides of the tunnel is larger when the rock mass quality decreases. Nevertheless, when the *GSI* values is over 60, the scatter range of δ value is more or less similar.

Fig. 10 presents the convergence displacement of points 1, 2 and 3 considering dip angle (β) and uniaxial compressive strength (σ_{ci}) variation while other parameters are fixed (*GSI* = 40, GSI_{tab} = 50). The influence of the dip angle (β) on the convergence displacement at point 2 is significant in the case of weak rock masses (σ_{ci} < 35 MPa). When the uniaxial compressive strength (σ_{ci}) increases, its influence decreases. The same results are however not observed for points 1 and 3. It can also be seen from **Fig. 10** a considerable effect of the compressive strength of the rock mass on the convergence displacements of points 1, 2 and 3 when σ_{ci} value is smaller than 35 MPa. The results obtained for other rock masses qualities in terms of *GSI* values are more or less similar to the case mentioned above. For the sake of simplicity, these results are therefore not presented.

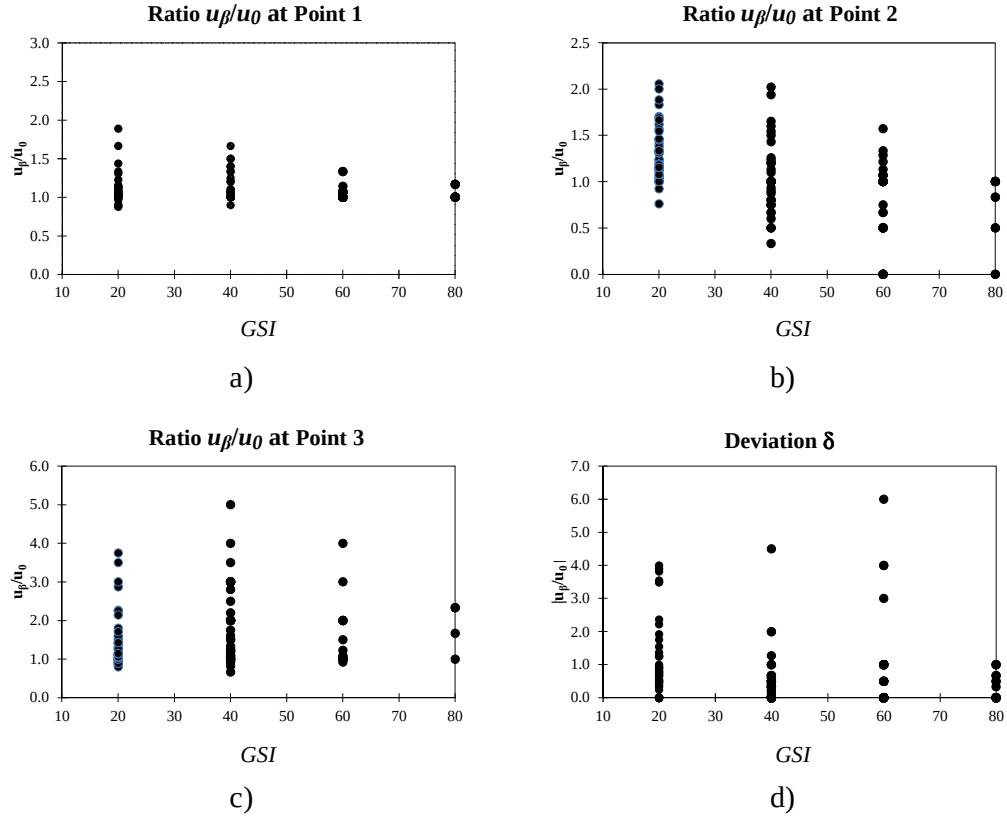

Fig. 9. Distribution of the ratio u_β/u_0 as a function of rock mass quality in terms of GSI for the case of an unsupported tunnel

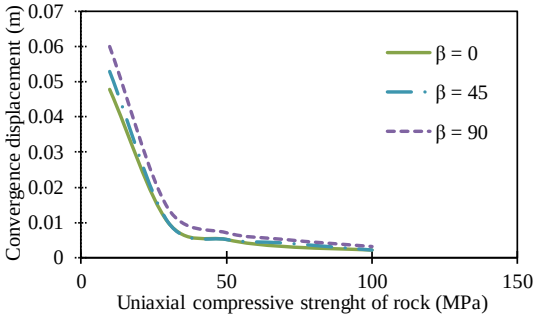

a) Convergence of point 1

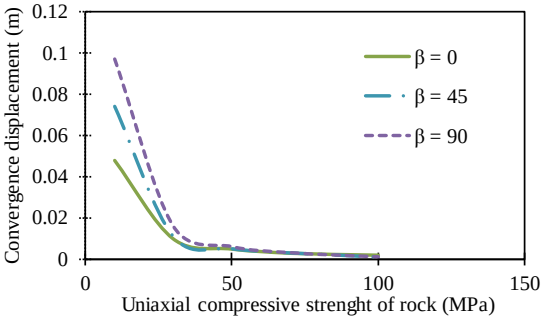

b) Convergence of point 2

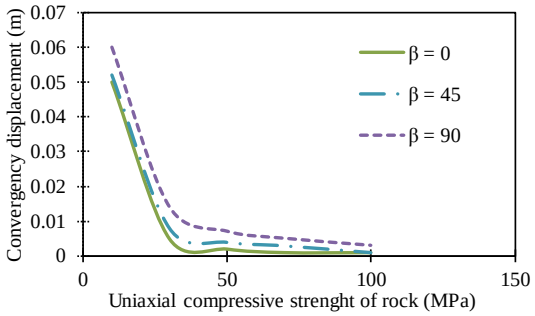

c) Convergence of point 3

Fig. 10. Convergence displacements of points 1, 2 and 3 considering the change in dip angle (β) and the uniaxial compressive strength (σ_{ci}) (GSI = 40, GSI_{tab} = 50) for the case of an unsupported tunnel

Fig. 11 presents the effect of the lateral earth pressure coefficient K_0 on the convergence displacement induced on the tunnel wall. Considering the change of joints condition, two values of GSI_{tab} of 50 and 75 have been investigated which corresponds to k_n = 11,085 MPa/m, k_s = 4,435 MPa/m and k_n = 111,128 MPa/m, k_s = 44,450 MPa/m. Other parameters are GSI = 40, σ_{ci} = 30 MPa.

In the case of poor joints condition (GSI_{tab} = 50), the convergence displacement at point 2 considerably depends on the dip angle of rock layers when K_0 value is larger than unity (**Fig. 11**a). This dependency decreases with good joints condition (GSI_{tab} = 75) (**Fig. 11**b). Generally, the higher the lateral earth pressure coefficient K_0, the larger the convergence displacement at point 2. The same dependency of the convergence displacement of the other points on the tunnel boundary is also observed.

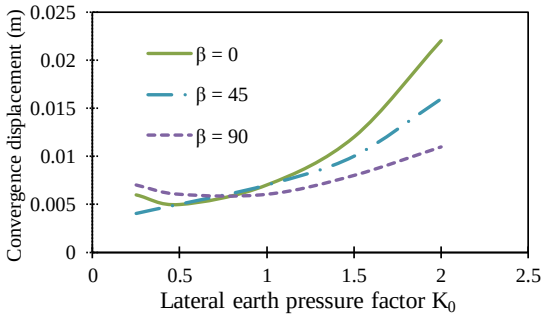

a) Convergence of Point 2 (GSI_{ref}= 40, σ_{ci}= 50, GSI_{tab}= 50)

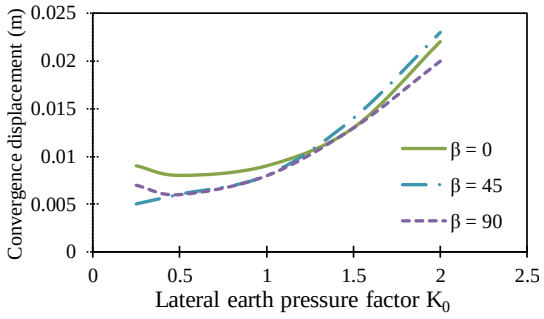

b) Convergence of Point 2 (GSI_{ref}= 40, σ_{ci}= 50, GSI_{tab}= 75)

Fig. 11. Convergence displacements at points 2 considering the change in the lateral earth pressure coefficient (K_0) and dip angle (β) (GSI = 40, σ_{ci} = 30 MPa) for the case of unsupported tunnel

5. Tunnels with support

Support structure of steel ribs type is widely used to support the tunnel excavated through inclined stratified rock mass in the Quangninh coal mine area. Parameters of the reference case has been adopted to analysis the influence of joints on the behavior of supported tunnels. Tunnels are located at the depth of 300 m from the ground surface. Joint spacing is equal to 1.0 m. The lateral earth pressure coefficient (K_0) is 0.5. Other parameters of rock mass and discontinuities are presented in **Table 6**. Properties of steel ribs are shown in **Table 4**.

Fig. 12 presents the distribution of yielded zones developed without and with support structure. It can be seen that the support structure has a great effect on the yielded zone range. As predicted, a smaller area of yielded zones is observed in the case of support.

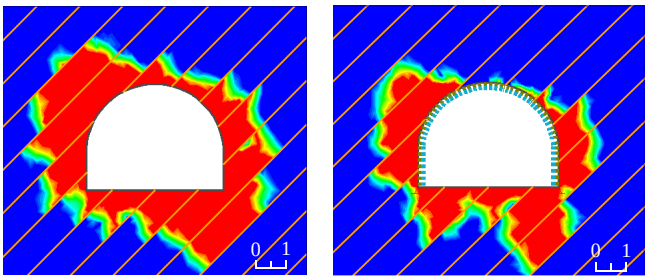

a) b)

Fig. 12. Yielded zones around tunnels (*GSI* = 40, GSI_{tab} = 50, σ_{ci} = 30 MPa, $\beta = 45^0$): (a) tunnel without support; (b) tunnel with support

Obviously, the support structure plays a role in reducing the deformation and/or the displacements of the rock mass. The development of yielded zones is therefore reduced. In addition, support structure causes reaction forces which helps to increase the radial stresses in the rock mass, i.e. the minor stress σ_3 (**Fig. 13**). Consequently, a triaxial stress state surrounding the tunnel is maintained and helps to mobilize the self-support capacity or the stability of the rock mass.

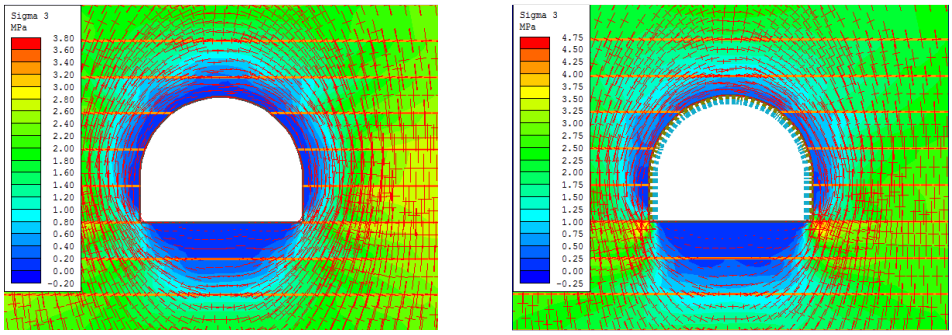

a) b)

Fig. 13. Minor principal stress (σ_3) in the rock mass: (a) tunnel without support; (b) tunnel with support ($\beta = 0^0$)

The influence of the support structure on the tunnel wall radial displacement is presented in **Fig. 14**. The displacements induced in the case of tunnel with support are smaller than the ones observed in the case of tunnel without support. However, when the uniaxial compressive rock mass strength σ_{ci} is greater than 35 MPa, the radial displacements difference in these two cases is negligible and is generally smaller than 1 cm (see **Fig. 14**). The support structures play an insignificant role in controlling the displacement of strong rock mass ($\sigma_{ci} \geq 35$ MPa in this study).

nvergence displacement (m)

nvergence displacement (m)

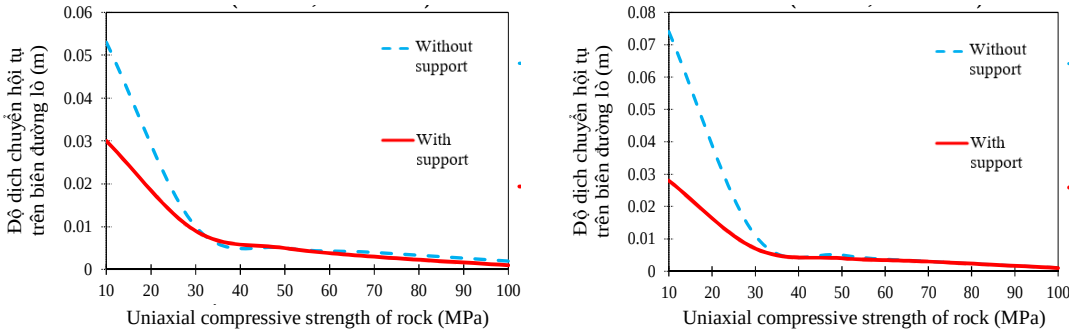

Fig. 14. Convergence displacement of tunnel without support (a) and tunnel with support (b) (GSI = 40, GSI_{tab} = 50, β = 45^0)

Fig. 15 presents the dependency of the ratio u_β/u_0 with the dip angle of rock layers. It is necessary to note that the results presented in **Fig. 15** includes all considered GSI values. It is similar to the investigated results obtained in the case of unsupported tunnels, the scatter of the ratio u_β/u_0 tends to increase for larger dip angles of rock layers. The larger the dip angle of rock layers, the greater the influence of joints in rock masses on the radial displacements. It is evident that the support structure does not significantly change the distribution of the ratio u_β/u_0.

Using the same numerical data from **Fig. 15**, **Fig. 16** presents the range of u_β/u_0 ratio with different GSI values. It can be seen from **Fig. 16** that the smaller the GSI value, the more dependence of u_β/u_0 ratio on the dip angle of rock layers. The same conclusion is obtained by the case of unsupported tunnel mentioned in section 4.

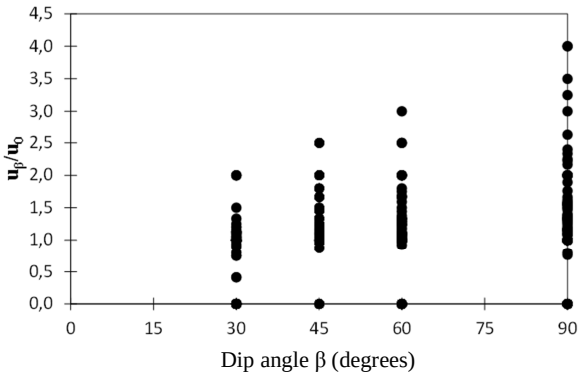

Fig. 15. Distribution of the ratio u_β/u_0 as a function of the dip angle (β) for the case of a supported tunnel without differentiation of GSI values

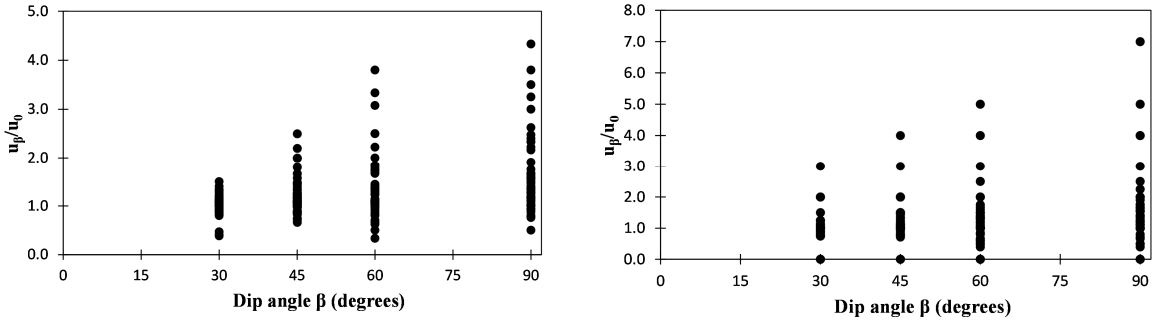

a) GSI = 20

b) GSI = 40

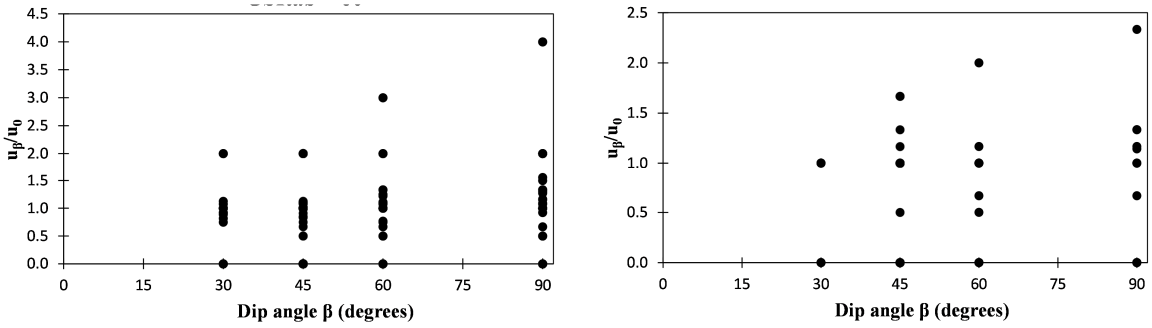

c) GSI = 60 d) GSI = 80

Fig. 16. Distribution of the ratio u_β/u_0 as a function of dip angle (β) for the case of a supported tunnel with differentiation of GSI values

In order to highlight the mechanism of deformation/displacement of the rock layers considering the effect of the lateral earth pressure coefficient (K_0) and of the dip angle of the rock layers (β) (**Fig. 5**), the deviation δ is presented in **Fig. 17**. Five different values of K_0 have been considered. Other parameters of the rock masses of the reference case have been adopted.

When the K_0 value is smaller than unity (i.e., K_0 = 0.25, 0.5) and the dip angle (β) is approximately smaller than 45 degrees, bending displacements are induced at point 2, which makes a perpendicular direction with the joint surface, is more predominant compared to the sliding displacements induced at point 3. On the other hand, when the dip angle (β) is approximately greater than 45 degrees, the larger displacements are observed at point 3 instead of point 2, which indicates the greater predominance of the sliding mechanism along the joint surface.

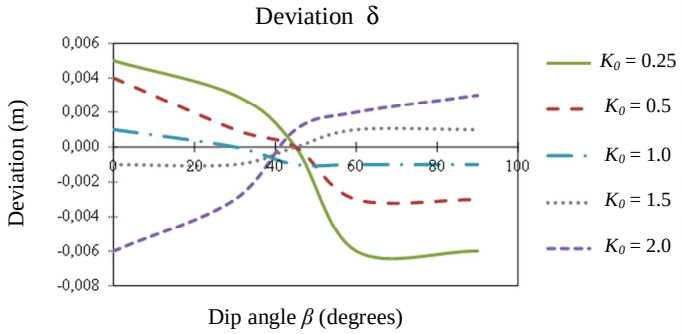

Fig. 17. Deviation of the convergence displacements at point 2 and point 3 considering different K_0 values (GSI = 40, σ_{ci} = 30 MPa, GSI_{tab} = 50) for the case of supported tunnel

For other cases of K_0 which are higher than unity (i.e., K_0 = 1,5 and 2), an opposite influence of K_0 on the deformation/displacement behavior of point 2 and point 3, is observed (**Fig. 17**). However, it should be noted that the predominant bending mechanism at point 2 or sliding mechanism at point 3 change at the critical dip angle of 45 degrees. It is reasonable to conclude that the smaller the angle (α) between the joint surface and the direction of the major principal stress, the more the sliding mechanism is predominant along the joint surface. On the other hand, bending displacements developed perpendicularly with the joint surface observed at point 2 will be greater than the sliding displacements at point 3 when the angle α increases.

Fig. 18 shows the yielded zone distribution for the reference rock with a dip angle of 45 degrees. It can be seen that, the failure area is complex and strongly dependent on the lateral

earth pressure coefficient K_0. In general, the smaller this coefficient is, the greater the yielded area is. Indeed, when the K_0 values are equal to 0.25 or 2, the yielded area is larger than the ones observed for K_0 values (i.e., K_0 = 0.5,1.0 and 1.5) (**Fig. 18**). It should also be noted that, the higher the K_0 value, the greater the yielded area, except for the case of K_0 value of 0.25. The main yielded area is located on the top left corner of the tunnel, while the small yielded area is observed on the top right corner.

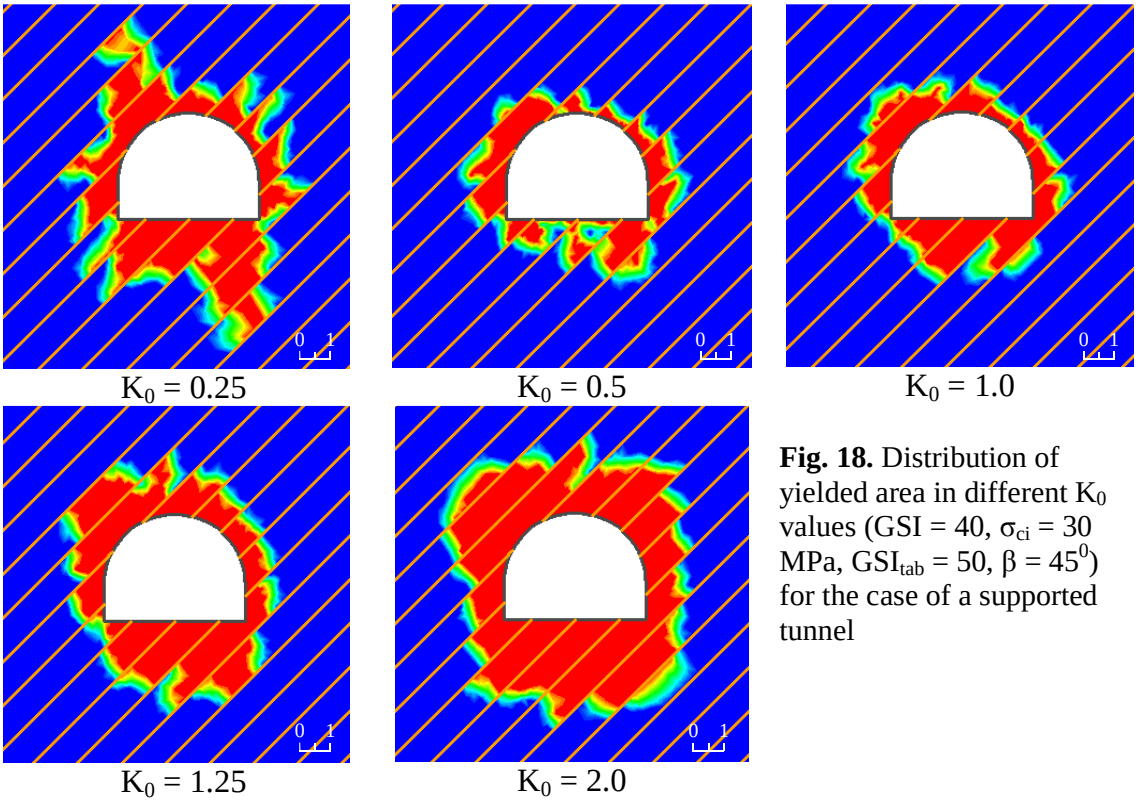

Fig. 18. Distribution of yielded area in different K_0 values (GSI = 40, σ_{ci} = 30 MPa, GSI_{tab} = 50, $\beta = 45^0$) for the case of a supported tunnel

5. Conclusions

In this study, numerical calculation has been conducted to investigate the effect of the dip angle, of the lateral earth pressure coefficient and of the rock mass quality on the convergence displacements of the surrounding rock mass. Some conclusions can be derived as follows:

- For intact rock masses without joints, the yielded zone is smaller than the one observed in the case of stratified rock masses. In addition, the stress distribution around the tunnel excavated in an isotropic rock mass and the case of horizontal and vertical stratification is symmetric. However, for the case of inclined stratified rock mass, the asymmetry of the yielded zone developed surrounding the tunnel increases gradually when the dip angle is greater.

- The convergence displacements induced in inclined layered rock masses are usually larger than the ones obtained in horizontally layered rock mass representing by the ratio u_β/u_0 which is usually larger than the unity. In addition, the smaller the GSI value, the more dependence of u_β/u_0 ratio on the dip angle of rock layers;

- An increase of the GSI value means an improvement of the rock mass quality and a decrease of the dependence of rock mass behavior on the discontinuities. Consequently, the scatter of the ratio u_β/u_0 tends to decrease as the GSI values increases;

- The deviation of convergences at two sides of the tunnel is larger when the stratified rock mass quality decreases. It means that the higher the *GSI* value, the smaller the deviation.

- For investigated cases in this study, when the uniaxial compressive rock mass strength σ_{ci} is greater than 35 MPa, the radial displacements difference in the two tunnel cases with

and without support structure is negligible. It means the support structures play an insignificant role in controlling the displacement of strong rock mass ($\sigma_{ci} \geq 35$ MPa in this study);

- The dip angle of the joint (β) of approximately 45 degrees could be considered as the critical angle at which displacement mechanism of rock mass changes between sliding and bending. When the K_0 value is smaller than unity (i.e., $K_0 = 0.25, 0.5$), bending mechanism is greatly developed at small dip angles (β) while sliding mechanism along the joint surface is more important at large dip angles (β). A sliding mechanism at small dip angle and bending mechanism at large dip angle, is observed for other cases of K_0 which are higher than unity.

ACKNOWLEDGMENTS: This research is funded by the Vietnamese National Foundation for Science and Technology Development (NAFOSTED) under grant number 105.08-2015.14. The license of Rocscience software at Hanoi University of Mining and Geology is appreciated.

REFERENCES

Barton N. A model study of rock-joint deformation. International Journal of Rock Mechanics and Mining Sciences 1972; 9: 579-602.

Barton N, Bandis S. Review of predictive capabilities of JRC-JCS model in engineering practice. International Symposium on Rock Joints, Loen 1990, 603-610.

Bobet A. Deep tunnel in transversely anisotropic rock with groundwater flow. Rock Mech Rock Eng 2016; 49: 4817-4832.

Do NA, Dias D, Oreste PP and Djeran-Maigre I. 2D Tunnel Numerical Investigation: The Influence of the Deconfinement method on Tunnel Behavior. Geotechnical and Geological Engineering 2014; 32(1): 43-58.

Fortsakis P, Nikas K, Marinos V, Marinos P. Anisotropic behavior of stratified rock masses in tunneling, Engineering Geology 2012; 141-142: 74-83.

Goodman RE. “Introduction to rock mechanics”, second ed. J. Wiley 1989, Chichester.

He B, Zhang Z, Chen Y. Unsymmetrical load effect of geologically inclined bedding strata on tunnels of passenger dedicated lines. Journal of Modern Transportation 2012; 20(1): 24-30.

Hoek E, Carranza-Torres C, Corkum B. Hoek-Brown failure criterion-2002 Edition, Proceedings of the 5th North American Rock Mechanics Symposium and the 17th Tunnelling Association of Canada: NARMS-TAC, Toronto, Canada 2002; 1: 267-273.

Hoek E, Diederichs MS. Empirical estimation of rock mass modulus. International Journal of Rock Mechanics and Mining Sciences 2006; 43: 203-215.

Institute of Mining Science and technology - Vinacomin (IMSAT). “Research on rock mass parameters in Quangninh coal area served to blasting, pressure control during minning”. Project report in Vietnamese 2012.

Jia P, Tang CA. Numerical study on failure mechanism of tunnel in jointed rock mass. Tunnelling and Underground Space Technology 2008; 23: 500-507.

Małkowski P. The impact of the physical model selection and rock mass stratification on the results of numerical calculations of the state of rock mass deformation around the tunnels. Tunnelling and Underground Space Technology 2015; 50: 365-375.

Marinos V. Tunnel behaviour and support associated with the weak rock masses of flysch. Journal of Rock Mechanics and Geotechnical Engineering 2014; 6: 227-239

Panthee S, Singh PK, Kainthola A, Singh TN. Control of rock joint parameters on deformation of tunnel opening. Journal of Rock Mechanics and Geotechnical Engineering 2016; 8: 489-498

Rafeh F, Mroueh H and Burlon S. Accounting for joints effect on the failure mechanism of shallow underground chalk quarries. Computers and Geotechnics 2015; 69: 247-261.

Rocscience. “Software Manual” (https://www.rocscience.com) 2016.

Tran MH, Sulem J, Subrin D. A closed-form solution for tunnels with arbitrary cross section excavated in elastic anisotropic ground. Rock mech. Rock Eng. 2015; 48: 277-288.

Yang H, Jiang X, Wen C, Yin J. Modeling the deformation of tunnel excavations in layered rock masses. Electronic Journal of Geotechnical Engineering 2013; 18: 723-734.

Wang M, Gou G, Wang X, Gou Y, Dao VD. Floor heave characteristics and control technology of the roadway driven. International Journal of Mining Science and Technology 2015; 25(2): 267-273.

Wang SY, Sloan SW, Tang CA, Zhu WC. Numerical simulation of the failure mechanism of circular tunnels in transversely isotropic rock masses. Tunnelling and Underground Space Technology 2012; 32: 231-244.

Highlights

- Effect of the lateral earth pressure coefficient and of the rock mass quality
- The stratification influence on the rock mass behavior is significant